

UNCLASSIFIED

AD NUMBER	
AD328815	
CLASSIFICATION CHANGES	
TO:	UNCLASSIFIED
FROM:	CONFIDENTIAL
LIMITATION CHANGES	
TO: Approved for public release; distribution is unlimited.	
FROM: Controlling DoD Organization: Department of Defense, Attn: Public Affairs Office, Washington, DC 20301.	
AUTHORITY	
NRO ltr dtd 19 Sep 2012; NRO ltr dtd 19 Sep 2012	

THIS PAGE IS UNCLASSIFIED

NOTICE: When government or other drawings, specifications or other data are used for any purpose other than in connection with a definitely related government procurement operation, the U. S. Government thereby incurs no responsibility, nor any obligation whatsoever; and the fact that the Government may have formulated, furnished, or in any way supplied the said drawings, specifications, or other data is not to be regarded by implication or otherwise as in any manner licensing the holder or any other person or corporation, or conveying any rights or permission to manufacture, use or sell any patented invention that may in any way be related thereto.

CONFIDENTIAL

CONFIDENTIAL

FILE COPY

Return to
ASTIA
ARLINGTON HALL STATION
ARLINGTON 12, VIRGINIA
Attn: TIRS

ATTACHED PAPER

LEFT ON DESK WHEN ROOM IS VACANT.

THESE PAPERS WILL BE RETURNED TO THE RESPONSIBLE CUSTODIAN EACH DAY.

353 600
DESTRUCTION CODE

R

APR 17 1962

~~CONFIDENTIAL~~

ASTIA FILE COPY

TITLE - (NOT TO EXCEED 40 LETTERS AND SPACES)

Dev. & Therml. Perform-Discoverer Ht. Shld.

DOCUMENT IDENTIFICATION NO.
62SD445

COPY NO.

212 OF 260 COPIES

ORIGINATED BY

DATE

Costello/Segletes 3/23/62

PAGES

23

CONTRACT NO.

LOCAL ACCOUNTABILITY NO.

LOGGED IN

LOGGED OUT

DATE

BY

DATE

BY

1

2

3

4

5

6

7

8

328 815

CONFIDENTIAL

CONFIDENTIAL

~~CONFIDENTIAL~~

LMSC 13 2748

DOCUMENT NO. 62SD445

**DEVELOPMENT AND THERMAL PERFORMANCE OF
THE DISCOVERER HEAT SHIELD**

BY

F.A. COSTELLO

J.A. SEGLETES

MISSILE AND SPACE VEHICLE DEPARTMENT
GENERAL  ELECTRIC

~~CONFIDENTIAL~~

ASTIA
APR 17 1962

TIA A

~~CONFIDENTIAL~~

DOCUMENT NO. 62SD445

This document contains 23 numbered pages.

Copy number 211 of 260 copies.

**DEVELOPMENT AND THERMAL PERFORMANCE OF
THE DISCOVERER HEAT SHIELD**

BY

F.A. COSTELLO

J.A. SEGLETES

To Be Presented At
LMSC Research Laboratories
Palo Alto, California

28 March 1962

EXCLUDED FROM AUTOMATIC RE-
GRADING; DOD DIR 5200.10 DOES
NOT APPLY

MISSILE AND SPACE VEHICLE DEPARTMENT
GENERAL  ELECTRIC
3190 Chestnut Street, Philadelphia 4, Penna.

~~CONFIDENTIAL~~

~~CONFIDENTIAL~~

ACKNOWLEDGEMENTS

The information contained within this report is the result of many hours of work by many people. The prime contributors toward this particular report are extended a special acknowledgement. Chief among these contributors were Messrs. T. Shaw, M. Di Giacomo, and W. Mertz.

~~CONFIDENTIAL~~

~~CONFIDENTIAL~~

TABLE OF CONTENTS

Section		Page
I	INTRODUCTION.	4
II	DESIGN CRITERIA AND PROCEDURES.	5
	Environment.	5
	Materials Considerations and Selections.	6
	Design Techniques.	7
III	CAPABILITY.	10
	Prediction.	10
	Verification.	11
IV	CONCLUSIONS.	12

LIST OF ILLUSTRATIONS

Figure		Page
1	Re-entry Vehicle Configuration.	13
2	Mark 4 Convective Heat Fluxes During Powered Flight (Hottest Case).	13
3	Comparison of Trajectories During Re-entry for Ballistic Missile and Discoverer Re-entry Capsule.	14
4	Comparison of Heat Fluxes During Re-entry for Ballistic Missile and Discoverer Re-entry Vehicle.	14
5	Gross Heat Fluxes for Discoverer Mark 4 During Re-entry (Hottest Case).	15
6	Convective Heat Flux Equations.	15
7	Angle of Attack Correction Factor Curves.	16
8	Effective Heat of Ablation of Phenolic Nylon.	16
9	Illustration of REKAP Analysis.	17
10	Heat Shield Thickness Definition.	17
11	Mark 4 Temperature and Charring Histories During Powered Flight.	18
12	Temperature Response of Surface 1 (Farthest from Earth).	18
13	Circumferential Temperature Distribution in Orbit.	19
14	Mark 4 Temperature and Charring Histories During Re-entry (Hottest Case). Data Calculated for Stagnation Point.	19
15	Mark 4 Temperature and Charring Histories During Re-entry (Hottest Case). Data Calculated for Beginning of Skirt.	20
16	Mark 4 Temperature and Charring Histories During Re-entry (Hottest Case). Data Calculated for End of Skirt.	20
17	Effect of Tolerances on Structure Temperature at Time of Parachute Deployment.	21
18	Schematic of Structural Test.	22

~~CONFIDENTIAL~~

~~CONFIDENTIAL~~

I. INTRODUCTION

The Discoverer re-entry vehicle, designed and developed by General Electric Company's Missile and Space Vehicle Department, under contract to Lockheed Missile and Space Company, was the first man-made object to be recovered from an orbital mission. The purpose of this paper is to present the considerations that influenced the design of the re-entry heat protection system as well as the methods employed in predicting and verifying the system performance capability.

The Discoverer heat protection system design was a pioneering effort. It involved a minimum-weight, highly efficient, and reliable design for a vehicle that was to be exposed to an environment that even today cannot be completely reproduced in simulators and large-scale air arc facilities.

Three significant phases are representative of the total environment to which the heat protection system was exposed: ascent heating, sustained hard vacuum, and re-entry heating. Of the high-temperature materials for the heat protection system that were considered for this environment, the ablation approach was found most satisfactory for minimum weight and efficient, reliable design.

Investigation of several classes of ablation materials showed that thermosetting plastics represented a practical design solution for re-entry satellite vehicles and that the "effective heat of ablation" concept is inadequate for accurate analysis of thermosetting plastic materials.

A review of all aspects of the Discoverer design is presented, including the environment definition, selection of the heat protection system, system design techniques, and the predicted vehicle capability. Significant advances that have been made in the system design technology for satellite heat protection since the inception of the Discoverer design are reviewed where applicable.

~~CONFIDENTIAL~~

~~CONFIDENTIAL~~

II. DESIGN CRITERIA AND PROCEDURES

The size, shape, and weight of the Discoverer re-entry vehicle were dictated by system requirements and booster capabilities. Preliminary design trade-offs determined that the configuration should be as shown in Figure 1. The shape is essentially a sphere-cone. Inside the heat shield, which is shown shaded, an aluminum capsule is housed. After vehicle re-entry, the parachute cover is ejected and the parachute deployed. The parachute drags the aluminum capsule out of the heat shield; the shield is discarded, and the aluminum capsule carries the payload safely to the impact area. It is with this configuration that the discussion will begin.

ENVIRONMENT

The re-entry capsule is subjected in succession to ascent heating, degassing in space, the hot and cold extremes of space, and re-entry heating. The ascent heating environment is adequately represented in terms of the aerodynamic heating rate as a function of time. This is shown in Figure 2 for the design, or maximum heating, trajectory. The gas cap thermal radiation flux is negligible.

During the orbital phase the prime environmental parameters of concern were the high vacuum and the low space temperature. The vacuum was of significance because it influenced the material selection in terms of outgassing rates. The space temperature was important because it contributed to low shield temperatures and, coupled with the sun, gave rise to large temperature gradients in the shield. Thermal stress problems resulted from the cold soak condition as well as the gradients.

The re-entry environments for the Discoverer vehicle represented a significant departure from those encountered by the ballistic missile re-entry systems. A comparison between trajectories of a typical low W/C_{DA} ballistic missile re-entry vehicle and the Discoverer vehicle is shown in Figure 3. For the satellite, deceleration occurs at comparatively high altitude. The differences between ICBM and satellite heating environments are partially illustrated in Figure 4. For equal ballistic factors and identical configuration and size, the peak heating rate is higher for the missile, but total heating is greater for the satellite because of the longer time involved. The longer heating pulse suggests that there will also be a longer time for the heat to penetrate the shield. Although aerodynamic heating prediction methods had been checked in X-17 Research Test Vehicle flights and verified at higher velocity in long-range ICBM heat-sink flights, similar results were not available for ablation material performance.

Figure 5 shows the predicted heat transfer to three locations on the Discoverer body for the design limit condition. The peak heat fluxes for the stagnation point, beginning and end of the conical skirt correspond to radiation equilibrium temperatures of 3780°R , 2640°R , and 2240°R , respectively ⁽¹⁾.

⁽¹⁾ The integrated fluxes are such that if they were used to evaporate water, they would require water blankets that were 2.8, 0.7, and 0.4 inches thick for the three points, taken in the same order.

~~CONFIDENTIAL~~

~~CONFIDENTIAL~~

MATERIALS CONSIDERATIONS AND SELECTIONS

The three general classes of materials considered on a preliminary basis for application to the Discoverer re-entry vehicle were metals, refractories, and plastics.

Metals

The use of metals for heat protection has been largely confined to heat-sink and radiative type systems. Heat-sink protection systems, which simply absorb the incident heat flux, are usable where both the heat transfer rate and integrated heat flux are small and weight is not a primary consideration. Radiative systems rely on high surface temperatures to reject the convective heating. Both the peak heating and integrated heating of the Discoverer design exceed the limits of efficient, lightweight, available metallic heat-sink or radiative systems.

Refractories

Refractory metals generally fall into the radiative class of heat protection systems. Graphite, however, combines the radiative property with mass transfer cooling due to its oxidation and sublimation. The injection of the carbon monoxide gas into the boundary layer "thickens" the boundary layer, reduces the temperature gradient at the wall, and thus decreases the heat input to the surface. Oxidation of the carbon in the boundary layer somewhat offsets the mass transfer cooling effect.

Quartz is another refractory that combines reradiation with mass transfer cooling and vaporization. Under high heat fluxes quartz softens, then vaporizes, at a very high temperature. There is no oxidation effect from the quartz injection into the boundary layer.

Unfortunately, graphite was still in the laboratory development stage at the time of the Discoverer design and thus could not be considered seriously for the short-range program. Quartz was found too heavy for the satellite re-entry application.

Plastics

There are basically two types of plastics that can be used for re-entry heat protection systems. One is the thermoplastic type, such as teflon, which is characterized by a decomposition process called depolymerization. The depolymerization process reduces complex hydrocarbon polymers to monomers, with a consequent absorption of heat. The monomer oxidizes and the gaseous products are injected into the boundary layer, providing mass transfer cooling. The second type of plastic is the thermosetting type, such as phenolic. A similar depolymerization process takes place, but instead of a complete removal of material, a solid residue is left behind in the form of a nonuniform cross-linked char sponge. The char acts as transpiration-cooled insulating layer.

An investigation of these plastics showed that the thermosetting type would best meet the weight and reliability requirements for the Discoverer heat protection system. The desirable thermosetting plastic thermodynamic properties sought in the ablation material were:

1. A low thermal diffusivity and depolymerization temperature, to minimize the amount of heat that is transferred into the structure.

~~CONFIDENTIAL~~

~~CONFIDENTIAL~~

2. The formation of a strong char layer with predictable properties.
3. The formation of a low-molecular-weight product to provide the most efficient mass transfer cooling agent.

Phenolic nylon was found to best meet the overall system requirements. The char layer formed by the nylon proved to be an efficient reradiation device; the degradation phenomena that occurred within the material provided an efficient means of absorbing the heat that did get through the char. This combination ablation-reradiation system was especially suitable for the re-entry satellite environment.

The load-carrying structure selected to back up the phenolic nylon ablation material was phenolic glass. This structure was carried over from earlier heat protection system designs, where the glass structure was found most reliable.

DESIGN TECHNIQUES

Ascent Flight

Because an orbit temperature control coating on the outside of the shield could be destroyed by ascent heating, the orbit design was based on bare-shield optical properties.⁽²⁾ Thus neither the high surface temperature during ascent nor the high outgassing rates of the hot shield nullified the orbit temperature control system. Outgassing effects were found insignificant with regard to shield performance when no coating was used.

Orbital Flight

The primary effect upon the shield during orbital flight was thermal stressing caused by large circumferential temperature gradients in the shield. The heat inputs consisted of direct solar radiation, albedo fluxes from the earth, and direct earth emission. Free molecule heating was insignificant, since the recovery capsule faced aft in the normal flight attitude. The orbits considered had perigee altitudes around 120 nautical miles. The incident radiant flux was determined using MSVD's Orbit Heat Flux program, which combines an oblate earth celestial mechanics program with the heat flux equations and geometry. The three-axes stabilization system is also used by this program. Shield temperature histories were calculated using a general three-dimensional transient conduction-radiation computer program that has been in operation at MSVD for several years.

Re-entry

It was found very early in the design that the most severe re-entry condition for the heat protection system occurred when the initial re-entry path angle was smallest, or, in other words, when the flight path at 325,000 feet was approximately 89 degrees from the downward vertical. The governing criteria were: (1) that the temperature of the structural phenolic glass liner be held below 900°F, and (2) that the temperature of the capsule mounting ring be held below 450°F. The requirement for the structure temperature was based on the combined aerodynamic and buckling acceleration loads. The ring temperature was based on the rigidity requirements of the explosive piston mounts.

⁽²⁾ Aerodynamic heating prediction methods are presented in the section on re-entry.

~~CONFIDENTIAL~~

~~CONFIDENTIAL~~

Laminar convective heat fluxes were calculated by Lees' classical solution of hypersonic heating, with properties evaluated at Eckert's reference enthalpy state as shown in Figure 6 (Ref. 1). For turbulent flow the heat prediction was based on a momentum integral technique suggested by Walker (Ref. 2). Both prediction methods have shown good agreement with long-range ICBM heat-sink data. Scala and Warren (Ref. 3) have since shown, both analytically and experimentally, that only for re-entry velocities much greater than 26,000 fps will the effect of ionization significantly modify the convection laws. In accordance with ICBM flight-test data, the transition from laminar to turbulent flow was based on a local Reynolds number of 200,000, which indicated that the flow was laminar throughout most of the flight. The inviscid flow field conditions were determined from MSVD's hypersonic flow field program for gases in chemical equilibrium (Ref. 4). Gas cap thermal radiation was determined using the same flow field and high-temperature air emissivity values, but was found to be only 1 percent of the convective flux. Nonequilibrium radiation becomes significant only at velocities well above 26,000 fps.

During re-entry, the vehicle motion is a result of combined spin and yaw. To account for the resultant angle-of-attack effects on aerodynamic heating, a correction factor, derived analytically and correlated with experimental data, was applied to the heat fluxes calculated for zero angle of attack. Figure 7 shows the correction factor $\bar{q}_\alpha \neq \bar{q}_\alpha = 0$ for the cyclic motion as a function of the maximum angle of attack for the three key body positions. The body orientation with respect to time was determined from six-degree-of-freedom trajectory analyses.

The thermostructural shield configuration and thickness was based on the established design criteria, and the convective and radiative heat inputs were determined for the maximum heat transfer or shallowest entry angle.

There were two approaches available for calculating the shield degradation and temperature response. The first was the seemingly crude approach of using an "effective heat-of-ablation," Q^* , in a conduction heat transfer analysis with the "conduction" temperature evaluated from ground data. Figure 8 shows one type of correlation of ICBM and ground-test data for spherical nose caps of phenolic nylon. It is noteworthy that a simple correlation of Q^* versus stagnation enthalpy would provide a reasonably good description of the complex transient phenomena of the reaction kinetics, the char formation, the gas flow through the char, and the mass ejection into the boundary layer. This correlation technique shows considerably more scatter when it is applied to the cone or cylinder sections of the vehicles, where the heat flux is low.

The second method for calculating the shield response took a completely different approach, using the MSVD REKAP analysis. The REaction Kinetics Ablation Program describes the entire physical process. Data taken from independent tests are used to determine the reaction rate constants, thermal conductivities, specific heats, and other pertinent physical property data for the shield material. The REKAP analysis uses this data in calculating the shield performance as shown in Figure 9, which illustrates the ablation process. The calculated heat flux is applied, mathematically, to the ablation material. As the temperature of the material rises, a reaction begins

(3) This is most plausible for the ICBM case shown, since mass addition is an important parameter on high-heat-transfer locations.

~~CONFIDENTIAL~~

~~CONFIDENTIAL~~

to take place whereby the material decomposes. The reaction proceeds until there are no reactants left, leaving behind a residue called char. In Figure 9 the reaction zone is at about the middle of the slab. Heat is applied to the material at the front face. The gas generated by the reaction passes through the char and blocks part of the convective heating. Some of the heat is radiated from the char surface. Of the heat that penetrates the char, most is absorbed in the gas flowing from the reaction zone. The apparent high specific heat of the gas is the result of the cracking processes taking place as the gas is heated. The heat that gets past the char layer is then split between the heat of formation of the gaseous products and the heat conducted through the virgin plastic toward the back face.

Both the Q^* and REKAP methods have been applied to ICBM designs being conducted at MSVD. In general the Q^* method has been found adequate for certain nose cap designs⁽⁴⁾ but too inaccurate for the low heat flux regions that are characteristic of low-heat-transfer regimes. Consequently, for the low flux regions, relatively large safety factors are required if the Q^* method is used. The REKAP analyses, on the other hand, have shown excellent correlation on all parts of the body.

Since the REKAP was in its initial development at the time of the Discoverer design, the less accurate Q^* method was used. As much ground-test data as could be generated was used to reduce safety factors to a minimum.

The shield thicknesses that resulted from the design study are shown in Figure 10. These are the thicknesses that will be considered in the discussion of the capability.

⁽⁴⁾ These designs are characterized by large loss of mass and dimensional change.

~~CONFIDENTIAL~~

~~CONFIDENTIAL~~

III. CAPABILITY

PREDICTION

Ascent Flight

As implied in the few statements concerning ascent heating, the ascent problems were essentially circumvented by the elimination of optical coatings for orbit temperature control. Figure 11 shows the outside surface temperature histories for the three key shield points. The point at which the flow turns laminar is apparent. Allowance was made in the orbital studies for the slight variation in infrared emissivity and solar absorptivity between the charred and uncharred materials.

Orbital Flight

A typical temperature history of a point on the conical section of the shield is shown in Figure 12. It can be seen from this figure that the effects of ascent heating are negligible after approximately the first orbit. The cyclic character of the curve is typical of transient responses from the satellite surface for flights alternately in the sun and in the shade. To illustrate the thermal gradient problem, Figure 13 shows the average shield temperature as a function of circumferential position. It was found necessary to cut the phenolic nylon with circumferential slots to overcome the bond line stresses.

Re-entry Flight

From the heat fluxes of Figure 5 the temperature and ablation histories shown in Figures 14, 15 and 16 were derived. The effective heat of ablation, Q^* , for the phenolic nylon was determined from the plot of Q^* vs h_g (enthalpy). Q^* was used as a constant in this analysis, based on the average enthalpy over the heating time. These responses are the result of the maximum heating trajectory that was anticipated, which was found to occur with the combination of a re-entry velocity of 26,370 fps at a path angle of 1.46 degrees, both measured at 325,000 feet altitude. Under minimum heating conditions, with a re-entry angle of 4.45 degrees, the integrated heat flux decreases by 40 percent, the heating time by 40 percent and the resultant depth of char by approximately 40 percent.

As in all design studies, one of the key questions is: What are the effects of the tolerances in thermophysical properties and variations in design due to manufacturing tolerances? To resolve this problem, a probability and error analysis was undertaken. The parameters studied are listed in Figure 17. This is an interesting analysis of the significance of each variable. In calculating the overall effect, it was assumed that the parameters are stochastically independent, that the effects of variations in the parameters on the structure temperature could be approximated by a linear relationship, and that the variations in values are normally distributed. The individual effects can be recognized on the chart. When the root-mean-square 3σ limit of structure temperature is determined using the information presented previously, it is obvious that the design is adequate and, in fact, can survive more extreme conditions than originally required. From another point of view, the vehicle could accept a greater payload and still survive 3σ conditions.

~~CONFIDENTIAL~~

~~CONFIDENTIAL~~

VERIFICATION

Ground Test

Ground test verification was provided by material tests, subsystem tests, and system tests. The material data were discussed in the section on design procedures, where the simple Q^* vs h_g plot was found to adequately correlate diverse test conditions, at least for high heat fluxes. The usual tests for other thermal properties were also conducted.

A structural subsystem test was performed to ensure the adequacy of the design under the high re-entry temperatures. Figure 18 shows a schematic of the test arrangement. The shield was bared to the phenolic glass structural liner; the degraded structural properties of the hot phenolic nylon left it with no load-carrying capability. The design conditions for the structural test were those corresponding to the time of parachute deployment. It was from this test that the liner temperature limit of 900°F was derived.

Several heat transfer tests of complete heat shields were attempted but there was little useful data obtained. The main difficulty in these tests was adequate simulation of the environment.

The low-temperature capability of the shield was verified in cold soak tests. The adequacy of the design to withstand the temperature gradients experienced in orbit was checked in the Lockheed Bemco High-Altitude Thermal Simulator Chamber. Thus thermal tests were directed primarily toward material studies, the structural test provided verification of the design limits, and the system tests were of the go/no-go type.

Flight Tests

No flight-test data have been obtained on the performance of the phenolic nylon shield. No shield instrumentation was allowed on the flight vehicles; however, judging from the maintenance of internal temperatures within the prescribed limits, it can be concluded that the design is adequate.

~~CONFIDENTIAL~~

~~CONFIDENTIAL~~

IV. CONCLUSIONS

The discussion of the limited test verification of the design capability concludes the design review that encompassed the environment definition, the material selection, the design procedures, and the design capability.

The end results of this design effort can now be considered. First of all, of course, increased confidence has been gained in design capability; but the main conclusions to be drawn are the two mentioned at the outset of this discussion: (1) the suitability of thermosetting plastics to satellite re-entry heat protection systems; and, (2) the inadequacy of the Q^* method of analysis.

The advantage of the thermosetting plastics lies mainly in the char formation and high reradiation from the char surface. The need for improved thermosetting materials, both with regard to performance and cost, has led General Electric to the development of castable ablation materials. The casting process has considerably reduced manufacturing costs, while the incorporation of additives and reinforcements has permitted tailoring of the materials to the application.

The development of the REKAP analysis has resulted in a detailed understanding of the ablation phenomena. It has permitted the correlation of many diverse test data. And, since it calculates the heat protection provided by each portion of the ablation process, it has proved invaluable in the development of new materials.

In addition to the development of the REKAP, two other computer programs have proved essential in the design of this satellite system. MSVD's Orbit Heat Flux Program was developed to handle the many combinations and permutations of orbit trajectories that had to be evaluated in analyzing the system. Its use has provided exact design conditions as well as the probability of encountering any given set of conditions. It has thus prevented overdesign, with its concurrent weight penalties, by permitting rapid determination of realistic, but extreme, design conditions.

Processes for configuration optimization were found to be amenable to mechanization. Consequently, a Configuration Selection Digital Computer Program was developed that optimizes the external shape, considering thermodynamics, aerodynamics, flight mechanics, weight and balance, and structural mechanics. Configurations belonging to certain families can be evaluated with this program at the rate of thousands per minute.

Thus, design capabilities have been extended by the development of computational techniques that now permit system optimization and detailed performance prediction.

~~CONFIDENTIAL~~

~~CONFIDENTIAL~~

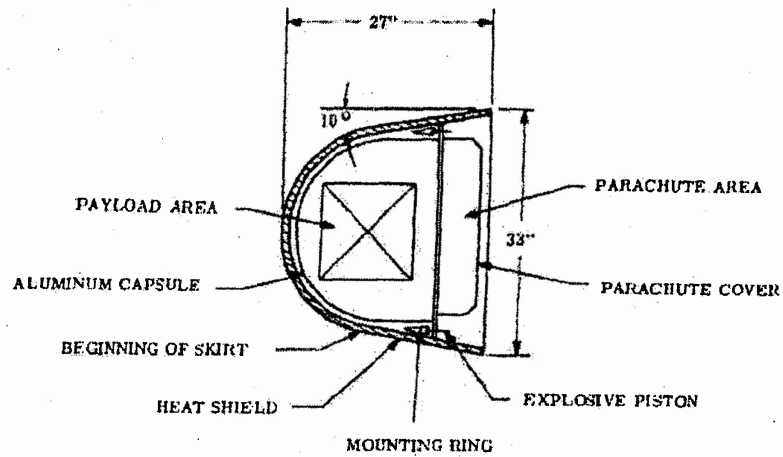


Figure 1. Re-entry Vehicle Configuration

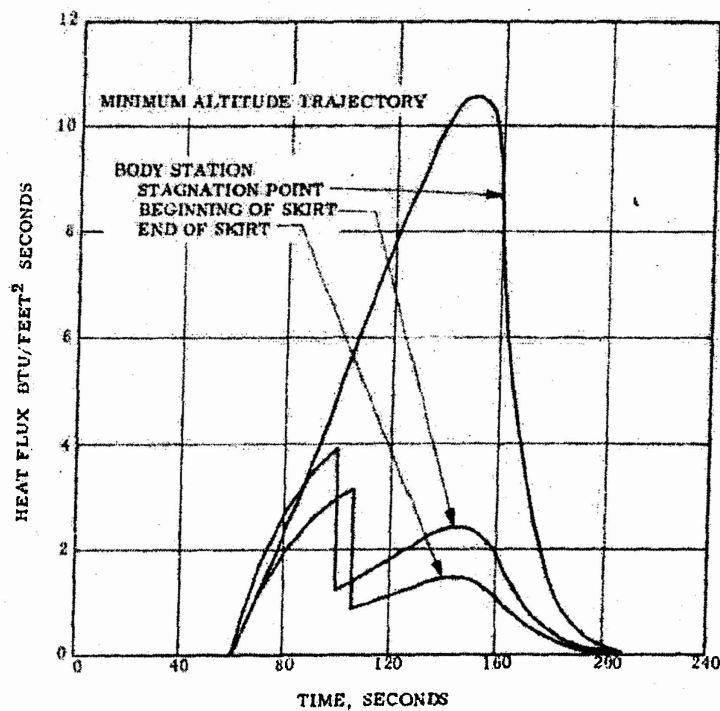


Figure 2. Mark 4 Convective Heat Fluxes During Powered Flight (Hottest Case)

~~CONFIDENTIAL~~

~~CONFIDENTIAL~~

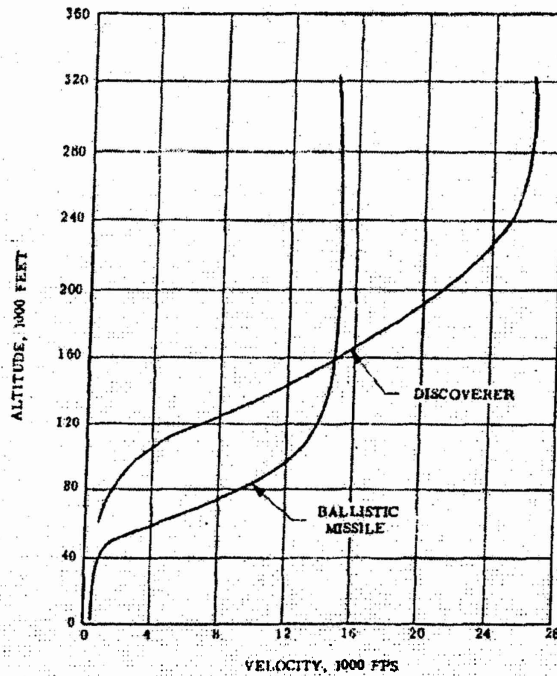


Figure 3. Comparison of Trajectories During Re-entry for Ballistic Missile and Discoverer Re-entry Capsule

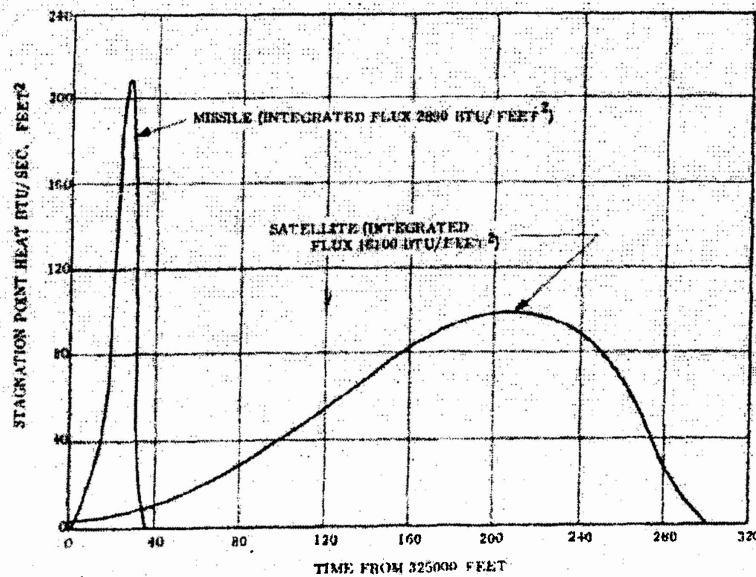


Figure 4. Comparison of Heat Fluxes During Re-entry for Ballistic Missile and Discoverer Re-entry Vehicle

~~CONFIDENTIAL~~

~~CONFIDENTIAL~~

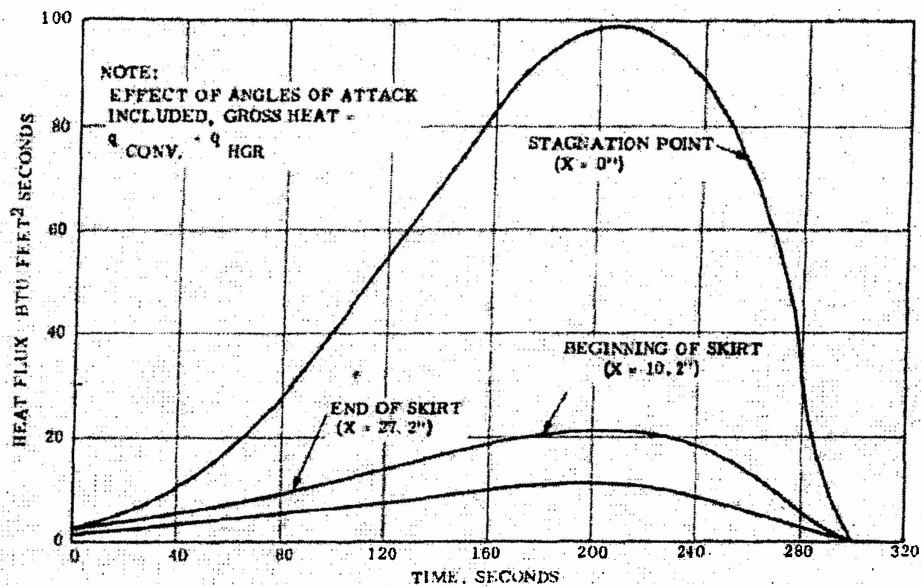


Figure 5. Gross Heat Fluxes for Discoverer Mark 4 During Re-entry (Hottest Case)

LAMINAR (LEES)

$$q_{stag} = \frac{0.760}{(Pr)^{2/3}} (\rho_e \mu_e U_o)^{1/2} (h_s - h_w)$$

$$q_{off\ stag} = \frac{0.389}{(Pr)^{2/3}} \frac{(\rho_e \mu_e U_o) y}{\left[\int_0^s (\rho_e \mu_e U_e y^2) ds \right]^{1/2}} (h_r - h_w)$$

TURBULENT (WALKER)

$$q = \frac{0.0296}{(Pr)^{2/3}} \frac{\rho_e \mu_e^{1/4} U_e \left(\frac{\mu_e}{\rho_e} \right)^{1/5} \left(\frac{\rho_e}{\rho} \right)^{4/5} y^{1/4}}{\left[\int_0^s \rho_e U_e \mu_e^{1/4} y^{5/4} ds \right]^{1/5}} (h_r - h_w)$$

Figure 6. Convective Heat Flux Equations

~~CONFIDENTIAL~~

~~CONFIDENTIAL~~

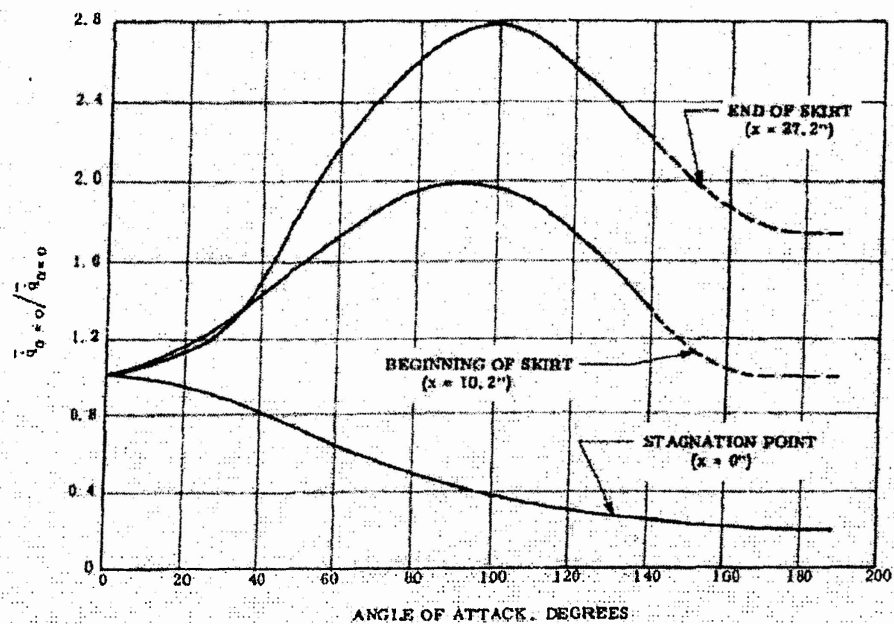


Figure 7. Angle of Attack Correction Factor Curves

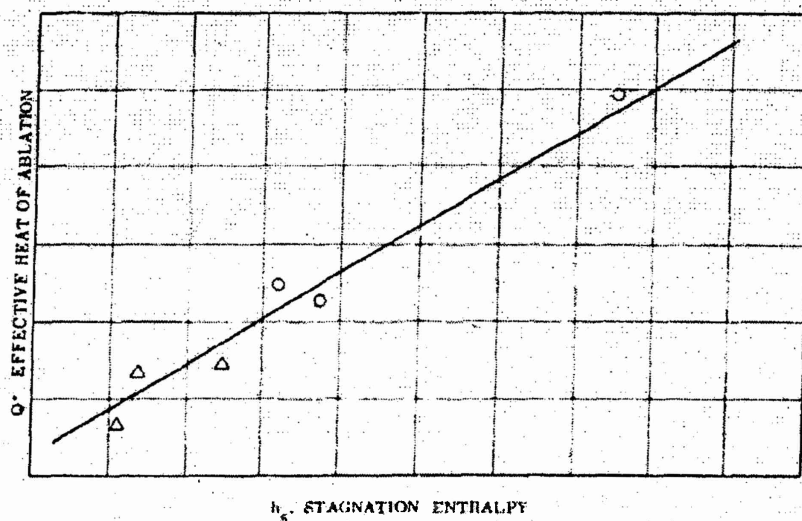


Figure 8. Effective Heat of Ablation of Phenolic Nylon

~~CONFIDENTIAL~~

~~CONFIDENTIAL~~

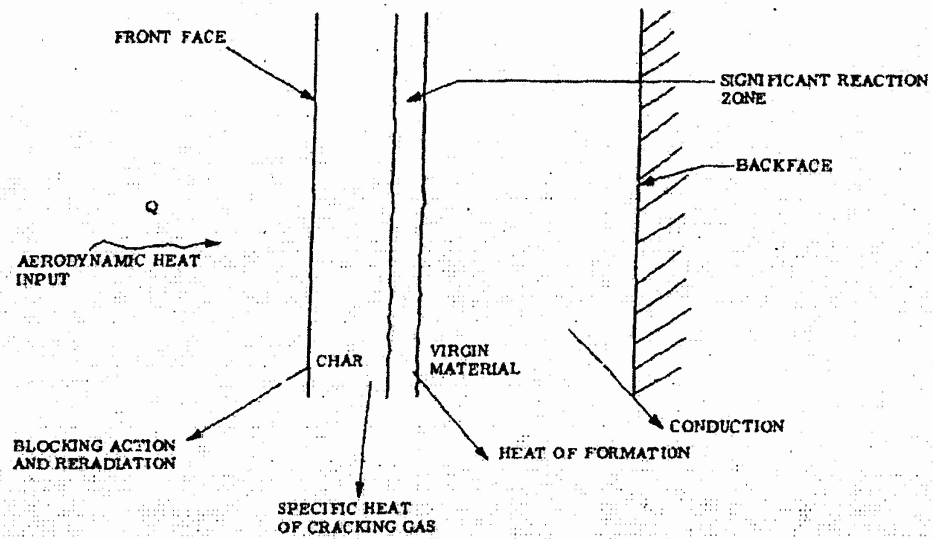


Figure 9. Illustration of REKAP Analysis

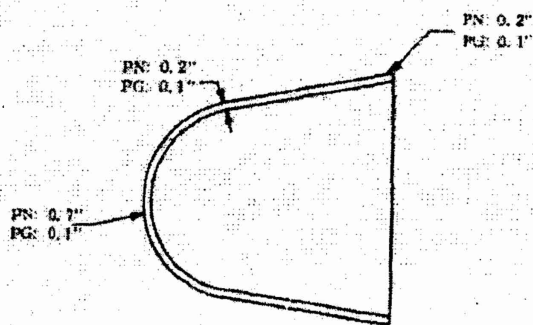


Figure 10. Heat Shield Thickness Definition

~~CONFIDENTIAL~~

~~CONFIDENTIAL~~

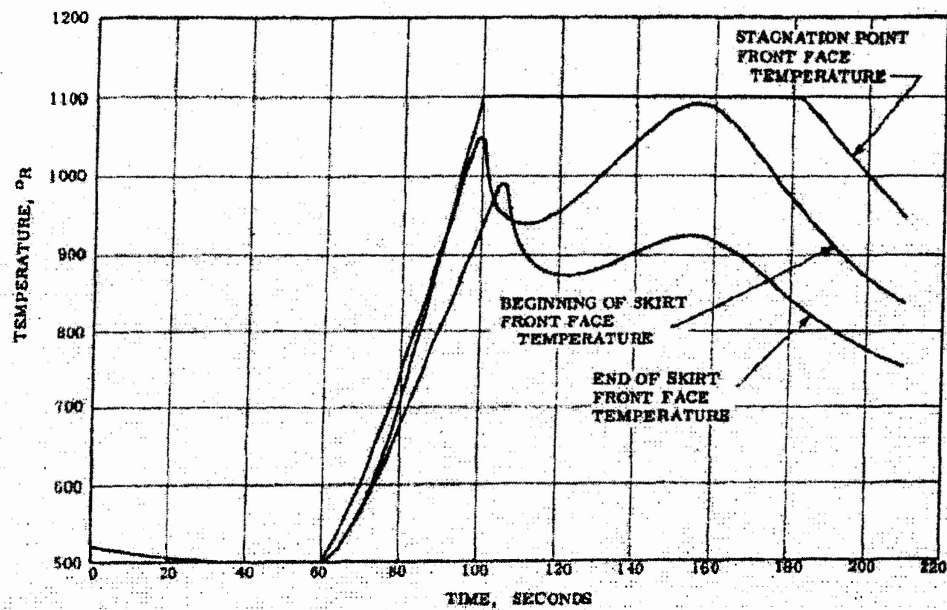


Figure 11. Mark 4 Temperature and Charring Histories During Powered Flight

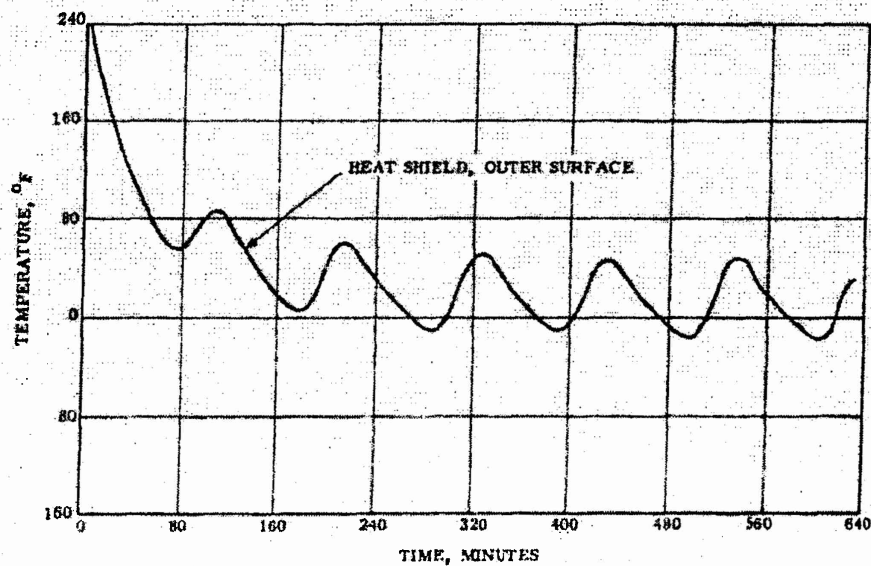


Figure 12. Temperature Response of Surface 1 (Farthest from Earth)

~~CONFIDENTIAL~~

~~CONFIDENTIAL~~

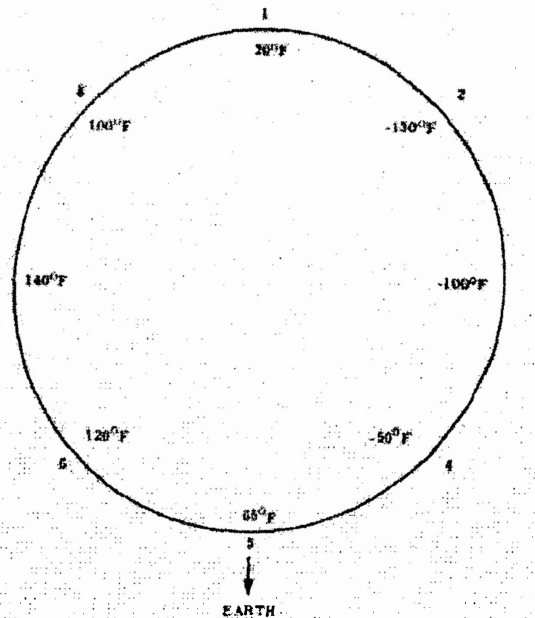


Figure 13. Circumferential Temperature Distribution in Orbit

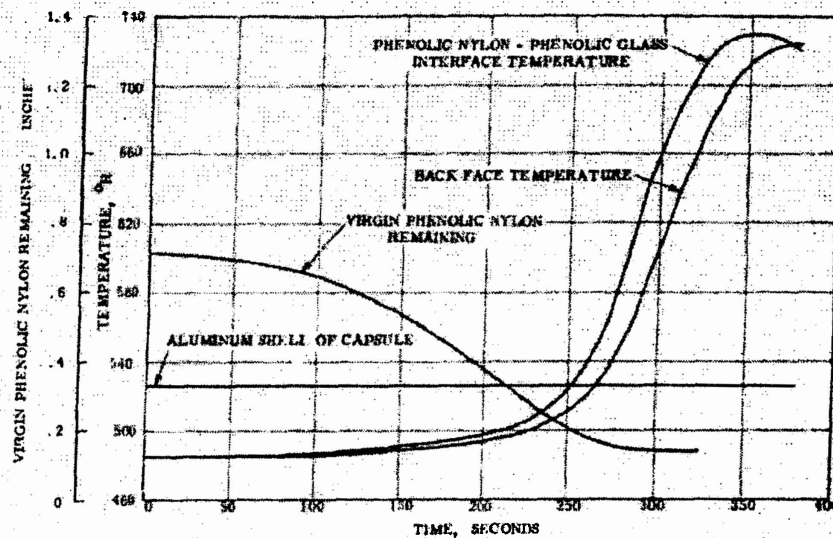


Figure 14. Mark 4 Temperature and Charring Histories During Re-entry (Hottest Case). Data Calculated for Stagnation Point.

~~CONFIDENTIAL~~

~~CONFIDENTIAL~~

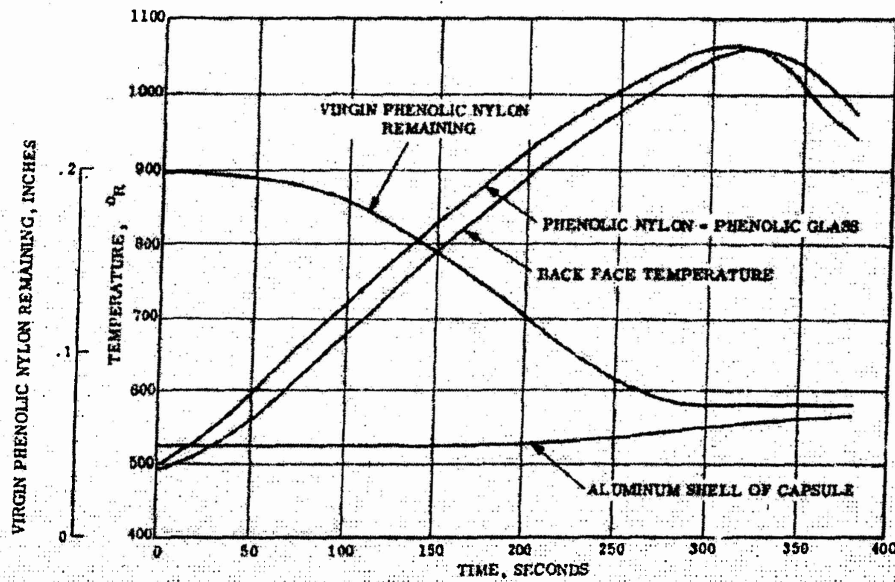


Figure 15. Mark 4 Temperature and Charring Histories During Re-entry (Hottest Case). Data Calculated for Beginning of Skirt.

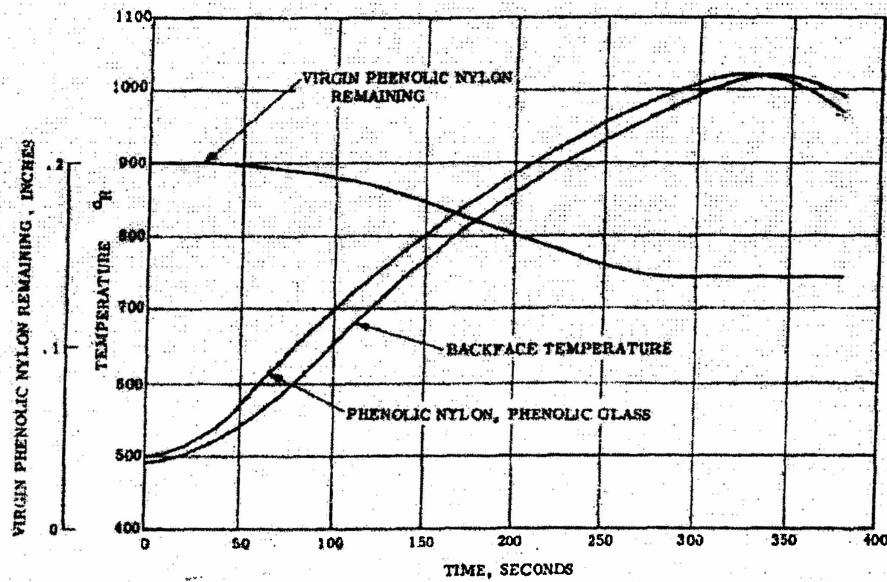


Figure 16. Mark 4 Temperature and Charring Histories During Re-entry (Hottest Case). Data Calculated for End of Skirt.

~~CONFIDENTIAL~~

CONFIDENTIAL

Parameter	Optimistic	Value of Parameter Nominal	Pessimistic	Stagnation Point	Temperature Effect (°F) Beginning of Skirt	End of Skirt
Path Angle - Degrees	4.61	3.1	1.90	-63	-45	-40
Initial Velocity - FT/SEC	25600	25685	28400	-6	-2	-8
Pitching Motion Envelope - Degrees				-1	-5	-8
Reynolds Number	300000	200000	50000	-1	-5	-8
Coef. of Heat Transfer exp. (distribution point)	.568	.780	.850	-10	0	0
(Laminar) at stag. pt.	.340	.399	.510	-15	0	-8
(Turbulent) at stag. pt.	.0237	.0296	.0335	-10	-6	-2
Weight - Lbs.	100	188	220	-10	-2	-8
Pressure Distribution				-1	-5	-8
Wall Temperature - °K	3000	2470	0	-3	-2	-1
Stagnation Point	3000	1660	0	-3	-2	-1
Skirt Region				-3	-2	-1
*Outer Layer Thickness - Inches - Stag. Point	.800	.715	.400	-20	-40	-20
*Skirt Region	.300	.199	.100	-13	-40	-20
*Outer Layer Density - LBS./FT ³	90	75	60	-3	-2	-2
*Outer Layer Conductivity BTU/FT ² SEC/°F/FT	.00003	.00004	.00008	-17	-5	-16
*Outer Layer Specific Heat BTU/LB - °K	.46	.40	.30	-6	-8	-1
*Inner Layer Thickness - Inches	.120	.105	.060	-5	0	-8
*Inner Layer Density - LBS./FT ³	130	120	80	-3	0	-12
*Inner Layer Conductivity BTU/FT ² SEC/°F/FT	.000040	.000085	.000090	-2	-3	-1
*Inner Layer Specific Heat - BTU/LB - °K	.32	.244	.23	-13	-19	-18
Latent Heat of Char - BTU/LB (based on grams lost)				-38	-5	-3
Charring Temperature - °K	950	1100	1250	-31	-99	-55
Drying Temperature at 3000 FT - °K	400	840	1100	-35	-9	-60
Initial Temperature - °K	440	540	640	-56	-12	-23

*Phenolic Nylon 38 - 45% Resin Content
 **Phenolic Glass 26 - 35% Resin Content

Figure 17. Effect of Tolerances on Structure Temperature at Time of Parachute Deployment

CONFIDENTIAL

~~CONFIDENTIAL~~

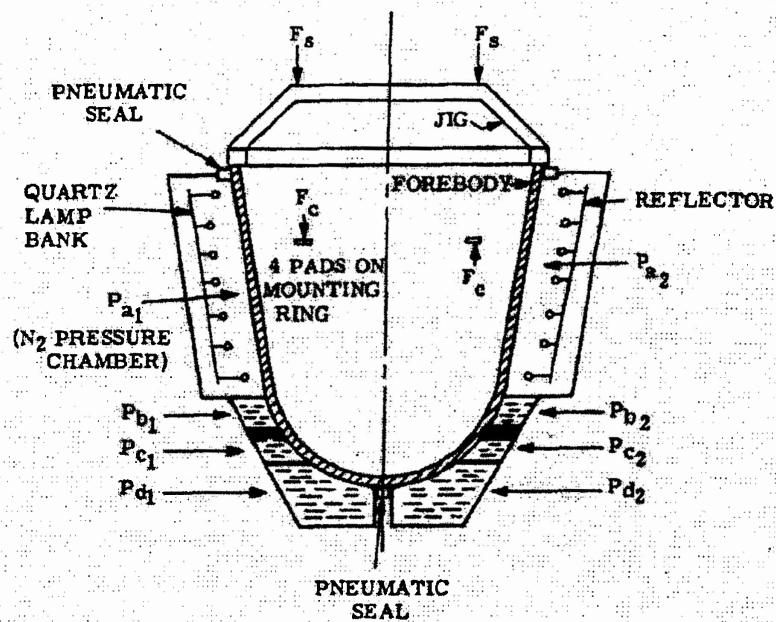


Figure 18. Schematic of Structural Test

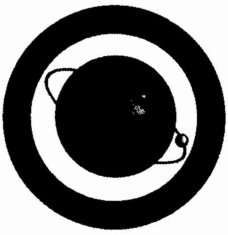
~~CONFIDENTIAL~~

~~CONFIDENTIAL~~

REFERENCES

1. L. Lees. Laminar heat transfer over blunt-nosed bodies at hypersonic flight speeds. Jet Propulsion, April 1956.
2. G. K. Walker. A particular solution to the turbulent boundary layer equations. Journal of Aerospace Sciences, Vol. 27, No. 9, September 1960.
3. S. M. Scala and W. R. Warren. Hypervelocity stagnation point heat transfer. General Electric Technical Information Series report R61SD185, October 1960.
4. F. Gravalos, I. Edelfelt, and H. Emmions. The supersonic flow about a blunt body of revolution for gases at chemical equilibrium. General Electric Technical Information Series report R58SD245, 16 June 1958.

~~CONFIDENTIAL~~



NATIONAL RECONNAISSANCE OFFICE

14675 Lee Road
Chantilly, VA 20151-1715

19 September 2012

Defense Technical Information Center
Attn: DTIC-OQ Information Security
8725 John J. Kingman Rd., Suite 0944
Ft. Belvoir, VA 22060-6218

To Whom It May Concern:

This concerns Technical Report AD-328815, ***Development and Thermal Performance of the Discoverer Heat Shield*** by F.A. Costello and J.A. Segletes.

Subsequent to National Reconnaissance Office (NRO) Freedom of Information Act request No. F12-0115, this record was approved for public release by the Acting Chief, Information Access and Release Team on 29 September 2012.

The attached declassified version of the document is now available for posting on the DTIC web site.

Please feel free to contact Linda Hall if you have any questions. She can be reached on 703 227-9158.

Sincerely,

A handwritten signature in black ink, appearing to read "Stephen R. Glenn".

Stephen R. Glenn, Chief
Information Management Services Center
Management Services and Operations
National Reconnaissance Office